

Eikonal Phase Shift Using Approximated Woods-Saxon Potential and its Application to the $^{12}\text{C} + ^{208}\text{Pb}$ Elastic Scattering

Yong Joo Kim*

Department of Physics, Cheju National University, Jeju 690-756

We presented the phase shift of Coulomb-modified eikonal model based on approximated Woods-Saxon potential. This phase shift has been applied satisfactorily to the analysis of elastic scattering of $^{12}\text{C} + ^{208}\text{Pb}$ system at $E_{lab} = 300$ and 420 MeV.

I. INTRODUCTION

Recently, considerable interest has been invested in the process of heavy ion elastic scattering. Heavy ion elastic scattering has been used as the starting point to understand more complicated reaction processes in heavy ion collisions. The outcome of elastic scattering data analysis generally is required to begin studies of other reaction. Differential elastic scattering cross sections have been measured for a large number of heavy ion systems. A number of studies [1-6] have been made to describe a heavy ion elastic scattering. The interpretation and description of elastic scattering phenomena in heavy ion reactions has been greatly facilitated through the application of the semiclassical method. In order to understand and analyze the elastic scattering data, various semiclassical models have been used.

The widely used semiclassical method for analysis of elastic scattering data is the WKB approximation [7]. The eikonal phase shift is derived from the integral equation by further approximating the WKB results. At high energies, the eikonal model has been employed in the analysis of the elastic scattering. The eikonal model has been found to be a convenient tool to describe the heavy ion elastic scattering. There has been a great deal of efforts [8-14] in describing elastic scattering processes between heavy ions within the framework of eikonal model. Ingemarsson *et al.* [11, 13] has discussed the effects of the real potential on the absorption of lighter heavy ions using "effective potential". The use of the distance of closest approach as an effective impact parameter in the eikonal formula provides a simple and efficient way to study heavy ion elastic scattering at relatively low energies. Different schemes devised to extend the eikonal approximation to the regime of low bombarding energies in heavy-ion collisions have been discussed [14]. Cha and Kim [15] have presented the first- and second-order corrections to the zeroth-order eikonal phase shifts for heavy-ion elastic scattering based on Coulomb trajectories of colliding nuclei and it has been applied to the $^{16}\text{O} + ^{40}\text{Ca}$ and $^{16}\text{O} + ^{90}\text{Zr}$ systems at $E_{lab} = 1503$ MeV. In recent, the $^{12}\text{C} + ^{12}\text{C}$, $^9\text{Li} + p$ and $^{11}\text{Li} + p$ elastic scatterings have been analyzed by Coulomb-modified eikonal model formalism based on hyperbolic trajectory

[16, 17].

Elastic scattering angular distributions for $^{12}\text{C} + ^{208}\text{Pb}$ system were measured for projectile energies between 10 and 35 MeV/nucleon and analyzed by optical model [18]. Total reaction cross sections of this system were extracted by an optical model analysis and compared to the prediction of the Glauber model. In this paper, we present the phase shift of Coulomb-modified eikonal model based on approximated Woods-Saxon potential and apply it to the elastic scattering of $^{12}\text{C} + ^{208}\text{Pb}$ system at $E_{lab} = 300$ and 420 MeV, respectively. In the following section, we describe Coulomb-modified eikonal model formalism using approximated Woods-Saxon potential. Section III contains the results and discussions for application of this formalism. Finally, concluding remarks are presented in section IV.

II. THEORY

A first-order WKB expression for the nuclear elastic phase shifts δ_L , taking into account the deflection effect due to Coulomb field, is given by [8]

$$\delta_L = \int_{r_t}^{\infty} k_L(r) dr - \int_{r_c}^{\infty} k_c(r) dr, \quad (1)$$

where r_t and r_c are the turning points corresponding to the local wave numbers $k_L(r)$ and $k_c(r)$ given by

$$k_L(r) = k \left[1 - \left(\frac{2\eta}{kr} + \frac{(L + \frac{1}{2})^2}{k^2 r^2} + \frac{U_N(r)}{E} \right) \right]^{1/2}, \quad (2a)$$

$$k_c(r) = k \left[1 - \left(\frac{2\eta}{kr} + \frac{(L + \frac{1}{2})^2}{k^2 r^2} \right) \right]^{1/2} \quad (2b)$$

where η is the Sommerfeld parameter, and $U_N(r)$ the nuclear potential. In the high energy limit, we can consider the nuclear potential as a perturbation. Thus, the turning point r_t may be taken to be coincident with $r_c = \left\{ \eta + [\eta^2 + (L + 1/2)^2]^{1/2} \right\} / k$ and

$$\begin{aligned} k_L(r) - k_c(r) &= k_c(r) \left[1 - \frac{2\mu U_N(r)}{\hbar^2 k_c^2(r)} \right]^{1/2} - k_c(r) \\ &\simeq - \frac{\mu U_N(r)}{\hbar^2 k_c(r)}. \end{aligned} \quad (3)$$

*Electronic address: yjkim@cheju.ac.kr

If we substitute Eq.(3) into Eq.(1) and rearrange the terms, the nuclear phase shift can be written as

$$\begin{aligned}\delta_L(r_c) &\simeq \int_{r_c}^{\infty} [k_L(r) - k_c(r)] dr \\ &= -\frac{\mu}{\hbar^2 k} \int_{r_c}^{\infty} \frac{r U_N(r)}{(r^2 - r_c^2)^{1/2}} dr.\end{aligned}\quad (4)$$

Furthermore, we have adopted a cylindrical coordinate system and decomposed the vector \mathbf{r} as $\mathbf{r} = \mathbf{r}_c + z\mathbf{n}$ where the z component of \mathbf{r} lies along \mathbf{n} and \mathbf{r}_c is perpendicular to \mathbf{n} . We may, therefore, write Eq.(4) as

$$\delta_L(r_c) = -\frac{\mu}{\hbar^2 k} \int_0^{\infty} U_N(r) dz \quad (5)$$

with $r = \sqrt{r_c^2 + z^2}$

Suppose that the nuclear potential $U_N(r)$ has a Woods-Saxon form

$$U_N(r) = -\frac{V_0}{1 + \exp[(r - R_v)/a_v]} - i\frac{W_0}{1 + \exp[(r - R_w)/a_w]} \quad (6)$$

with $R_{v,w} = r_{v,w}(A_1^{1/3} + A_2^{1/3})$ and that we are interest in waves for which the Coulomb distance of closest approach r_c is greater than R_v and R_w . Then the Woods-Saxon potential can be approximated by an exponential shape

$$U_N(r) \approx V(r_c) \exp[-(r - r_c)/a_v] + iW(r_c) \exp[-(r - r_c)/a_w], \quad (7)$$

where

$$\begin{aligned}V(r_c) &= -V_0 \exp[(R_v - r_c)/a_v], \\ W(r_c) &= -W_0 \exp[(R_w - r_c)/a_w].\end{aligned}\quad (8)$$

Using Eq.(7), the ordinary Coulomb-modified eikonal phase shift $\delta_L(r_c)$ of Eq.(5) is written as

$$\delta_L(r_c) = -\frac{\mu}{\hbar^2 k} \left\{ V(r_c) \int_0^{\infty} \exp[-(r - r_c)/a_v] dz + iW(r_c) \int_0^{\infty} \exp[-(r - r_c)/a_w] dz \right\}. \quad (9)$$

Using the binomial expansion of

$$r = \sqrt{r_c^2 + z^2} = r_c \left(1 + \frac{z^2}{r_c^2} \right)^{1/2} \approx r_c + \frac{z^2}{2r_c}, \quad (10)$$

and substituting Eq.(10) into Eq.(9), the phase shift $\delta_L(r_c)$ becomes

$$\delta_L(r_c) = -\frac{\mu}{\hbar^2 k} \left\{ V(r_c) \int_0^{\infty} \exp\left[-\frac{z^2}{2r_c a_v}\right] dz + iW(r_c) \int_0^{\infty} \exp\left[-\frac{z^2}{2r_c a_w}\right] dz \right\}. \quad (11)$$

The integral part of above equation can be calculated as

$$\begin{aligned}\int_0^{\infty} \exp\left[-\frac{z^2}{2r_c a_v}\right] dz &= \sqrt{\frac{\pi r_c a_v}{2}}, \\ \int_0^{\infty} \exp\left[-\frac{z^2}{2r_c a_w}\right] dz &= \sqrt{\frac{\pi r_c a_w}{2}}.\end{aligned}\quad (12)$$

by using Gamma function. Accordingly, the ordinary Coulomb-modified eikonal phase shift $\delta_L(r_c)$ of Eq.(11) takes the form

$$\delta_L(r_c) = -\frac{\mu}{\hbar^2 k} \sqrt{\frac{\pi r_c}{2}} \{ \sqrt{a_v} V(r_c) + i\sqrt{a_w} W(r_c) \}. \quad (13)$$

The elastic scattering amplitude for spin-zero particle via Coulomb and short-range central forces is given by

$$f(\theta) = f_R(\theta) + \frac{1}{ik} \sum_{L=0}^{\infty} \left(L + \frac{1}{2} \right) \exp(2i\sigma_L) (S_L^N - 1) P_L(\cos \theta), \quad (14)$$

where $f_R(\theta)$ is the usual Rutherford scattering amplitude and σ_L the Coulomb phase shift. The nuclear S -matrix elements S_L^N in this equation can be expressed by the nuclear phase shift δ_L , so that

$$S_L^N = \exp(2i\delta_L). \quad (15)$$

TABLE I: Input parameters of Woods-Saxon potential for $^{12}\text{C} + ^{208}\text{Pb}$ system at $E_{lab} = 300$ and 420 MeV. Set I are our fitting parameters, while Set II are ones taken from Ref. [18].

E_{lab} (MeV)	V_0 (MeV)	r_v (fm)	a_v (fm)	W_0 (MeV)	r_w (fm)	a_w (fm)	
300	Set I	157	0.925	0.864	98	1.017	0.785
	Set II	95	0.868	1.168	250	0.985	0.662
420	Set I	192	0.925	0.860	116	1.003	0.807
	Set II	95	1.068	0.80	200	1.033	0.658

III. RESULTS AND DISCUSSIONS

As in the preceding section, we have applied phase shift Eq.(13) of eikonal model using approximated Woods-Saxon potential to the elastic scattering of $^{12}\text{C} + ^{208}\text{Pb}$ at $E_{lab}=300$ and 420 MeV, respectively. The measured differential cross sections for this system are divided by the Rutherford cross section and displayed by solid circles. Table I show the Woods-Saxon potential parameters obtained from eikonal model fit to the experimental data [18]. In figures 1 and 2, the elastic scattering cross section data of $^{12}\text{C} + ^{208}\text{Pb}$ at $E_{lab} = 300$ and 420 MeV are compared with the present results. In this figures, the solid curves are the our calculated results using the parameters (Set I) given in table I, while the dashed curves are those using Woods-Saxon potential parameters of the Sahn *et al.* (Set II in table I).

As shown in figures 1 and 2, our calculated results of Coulomb-modified eikonal phase shift using approximated Woods-Saxon potential are in quite good agreement with the observed data. The results of Sahn *et al.*'s parameters [18] also show the shape and trend of these cross sections. As a whole, two calculations reproduce structures and magnitudes of data over the whole angular ranges, although the results of Sahn *et al.*'s parameters underpredict slightly the data at $E_{lab} = 420$ MeV beyond 7° . Our calculations found using eikonal phase shift provide reasonable fit to the elastic cross section of $^{12}\text{C} + ^{208}\text{Pb}$ system at $E_{lab} = 300$ and 420 MeV.

The transmission functions of Coulomb-modified eikonal model using the potential parameters of Set I in table I, $T_L = 1 - |S_L^N|^2$, is plotted in figure 3 as a function of angular momentum L . The values of T_L are decrease rapidly in the narrow angular momentum zones around $T_L = 1/2$. As expected, the T_L of the $E_{lab} = 420$ MeV scattering is shifted toward higher momentum transfer values when compared with one of $E_{lab} = 300$ MeV. Such shift raise the values of critical angular momentum $L_{1/2}$ corresponding to $T_L = 1/2$. This improvement is also reflected in the strong absorption radius R_s from the simple relation $(L_{1/2} + 1/2) \simeq kR_s$, the distance where the incident particle has the same probability to be absorbed as to be reflected. The critical angular momenta $L_{1/2}$, the strong absorption radii R_s and total reaction cross sections σ_R are listed in table II.

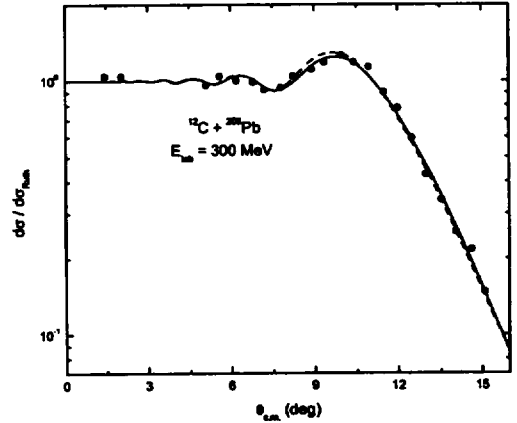

 FIG. 1: Elastic scattering angular distributions for the $^{12}\text{C} + ^{208}\text{Pb}$ system at $E_{lab} = 300$ MeV. The solid circles denote the observed data taken from Ref.[18]. The solid curve is the our calculated results (Set I in table I), while dashed curve is the calculated one (Set II in table I) using potential parameters taken from Ref.[18].

 TABLE II: Critical angular momenta ($L_{1/2}$), strong absorption radii (R_s) and reaction cross sections (σ_R) values from the eikonal model based on approximated Woods-Saxon potential for $^{12}\text{C} + ^{208}\text{Pb}$ system at $E_{lab} = 300$ and 420 MeV, respectively.

E_{lab} (MeV)	$L_{1/2}$	R_s (fm)	σ_{R_s} (mb)	σ_R (mb)
300	124	10.0	3162	3309
420	152	10.4	3390	3559

The strong absorption radius provides a good estimate of total reaction cross section in terms of $\sigma_{R_s} = \pi R_s^2$.

The removal of probability current in elastic scattering is related to the fact that processes other than elastic ones occur in a nuclear collision, which absorbed some of this current. A quantitative measure of the absorption is provided by the reaction or absorption cross section. The total reaction cross section for spinless nuclei is defined as

$$\sigma_R = \frac{2\pi}{k^2} \sum_{L=0}^{\infty} (2L+1)(1 - |S_L^N|^2). \quad (16)$$

This relationship establishes a link between the scattering and the reaction cross section. As shown in table II, total reaction cross section increases as incident energy increases. Our total reaction cross section calculations of eikonal model are fair agreement with the values of optical model analysis of Sahn *et al.* : $\sigma_R = 3236$ mb

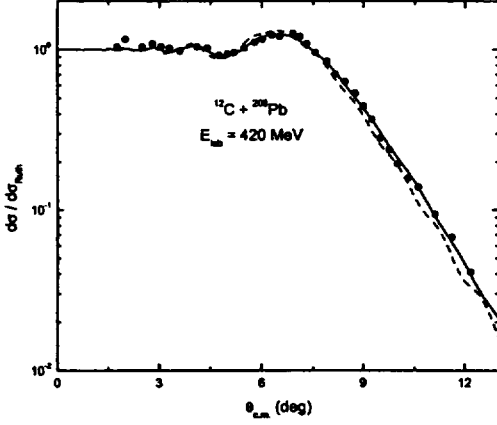


FIG. 2: Elastic scattering angular distributions for the $^{12}\text{C} + ^{208}\text{Pb}$ system at $E_{lab} = 420$ MeV. The solid circles denote the observed data taken from Ref.[18]. The solid curve is the our calculated results (Set I in table I), while dashed curve is the calculated one (Set II in table I) using potential parameters taken from Ref.[18].

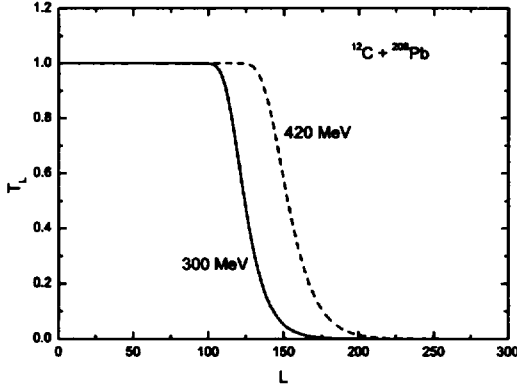


FIG. 3: Transmission functions T_L for $^{12}\text{C} + ^{208}\text{Pb}$ system at $E_{lab} = 300$ and 420 MeV, respectively.

(300 MeV) and 3561 mb (420 MeV).

Figure 4 shows the partial reaction cross section (using the potential parameter Set I in table I), $\frac{2\pi}{k^2} (2L+1)(1 - |S_L^N|^2)$, of $^{12}\text{C} + ^{208}\text{Pb}$ system at $E_{lab} = 300$ and 420 MeV, respectively, versus the orbital angular momentum L . As is well known, the reaction cross section is a quantitative measure of the absorption in a nuclear collision process that absorbs some probability current in elastic scattering. In figure 4, the partial reaction cross section is found to increase linearly up to $L = 107$ and 132 corre-

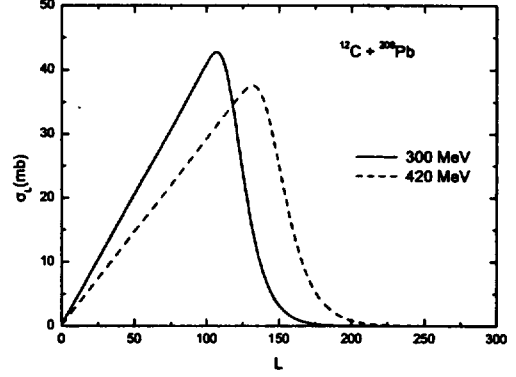


FIG. 4: Partial reaction cross section for the $^{12}\text{C} + ^{208}\text{Pb}$ system at $E_{lab} = 300$ and 420 MeV, respectively.

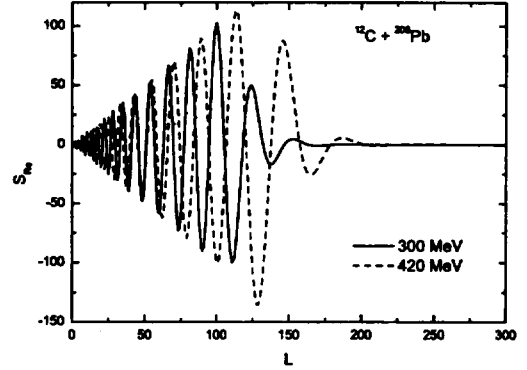


FIG. 5: Real part S_{Re} of $S = \frac{1}{2}(L+1/2) \exp(2i\sigma_L)(S_L^N - 1)$ for $^{12}\text{C} + ^{208}\text{Pb}$ system at $E_{lab} = 300$ and 420 MeV, respectively.

sponding to peak values of $\sigma_R = 43$ mb and $\sigma_R = 38$ mb for $E_{lab} = 300$ and 420 MeV, respectively, and by those peak values σ_R decrease quadratically to zero.

In order to investigate the partial wave contributions to the cross section in terms of orbital angular momentum L , we plot in figure 5 the real parts (S_{Re}) of the terms, $\frac{1}{2}(L+1/2) \exp(2i\sigma_L)(S_L^N - 1)$, which is included in scattering amplitude. As shown in this figure, S_{Re} show rapid variations in terms of L up to $L \sim 160$ and 200 for $^{12}\text{C} + ^{208}\text{Pb}$ system at $E_{lab} = 300$ and 420 MeV, respectively. By those L values, S_{Re} reduce to zero. We can see that the regions of higher partial waves give not nearly contribution to the scattering cross section.

IV. CONCLUDING REMARKS

In this paper, we have presented the phase shift of Coulomb-modified eikonal model based on approximated Woods-Saxon potential. It has been applied satisfactorily to the elastic scatterings of $^{12}\text{C} + ^{208}\text{Pb}$ system at $E_{lab} = 300$ and 420 MeV, respectively. The calculated differential cross sections lead to reasonable agreement with experimental data of this system. Total reaction cross section calculations of Coulomb-modified eikonal model are fair agreements with the values of optical model analysis.

Transmission functions T_L are decrease rapidly in the narrow angular momentum zones around $T_L = 1/2$. T_L

of the $E_{lab} = 420$ MeV scattering is shifted toward higher momentum transfer values when compared with one of $E_{lab} = 300$ MeV. The strong absorption distance provides a good measurement of total reaction cross section in terms of $\sigma_{R_0} = \pi R_0^2$. The values of partial wave reaction cross section increase linearly up to $L = 107$ and 132 for $E_{lab} = 300$ and 420 MeV, respectively. Beyond these L values, the partial reaction cross sections become quadratically to zero.

The use of phase shift expression based on the approximated Woods-Saxon potential in the Coulomb-modified eikonal model seems to be an alternative method to analyze the heavy ion elastic scattering.

-
- [1] M. Buenerd, A. Lounis, J. Chauvin, D. Lebrun, P. Martin, G. Duhamel, J. C. Gondrand, and P. De Saintignon, Nucl. Phys. A **424**, 313 (1984).
- [2] M. E. Brandan, Phys. Rev. Lett. **60**, 784 (1988).
- [3] D. T. Khoa, W. von Oertzen, H. G. Bohlen, G. Bartsch, H. Clement, Y. Sugiyama, B. Gebauer, A. N. Ostrowski, Th. Wilpert and C. Langner, Phys. Rev. Lett. **74**, 34 (1995).
- [4] M. P. Nicoli, F. Haas, R. M. Freeman, N. Atsacou, C. Beck, A. Elanique, R. Nouicer, A. Morsad, S. Szilner, Z. Basrak, M. E. Brandan, and G. R. Satchler, Phys. Rev. C **60** 064608 (1999).
- [5] Dao T. Khoa, W. von Oertzen, H. G. Bohlen and F. Nuoffer, Nucl. Phys. A **672**, 387 (2000).
- [6] A. Ingemarsson and M. Lantz, Phys. Rev. C **72**, 064615 (2005).
- [7] T. W. Donnelly, J. Dubach and J. D. Walecka, Nucl. Phys. Nucl. Phys. A **232**, 355 (1974).
- [8] C. K. Chan, P. Suebka and P. Lu P, Phys. Rev. C **24**, 2035 (1981).
- [9] D. M. Brink, "Semi-Classical Methods for Nucleus-Nucleus Scatterings", Cambridge University Press. (1985)
- [10] F. Carstou and R. J. Lombard, Phys. Rev. C **48** 830 (1993).
- [11] A. Ingemarsson and G. Faldt, Phys. Rev. C **48**, R507 (1993).
- [12] S. M. Eliseev and K. M. Hanna, Phys. Rev. C **56**, 554 (1997).
- [13] A. Ingemarsson, Phys. Rev. C **56**, 950 (1997).
- [14] C. E. Aguiar, F. Zardi, and A. Vitturi, Phys. Rev. C **56**, 1511 (1997).
- [15] M. H. Cha and Y. J. Kim, Phys. Rev. C **51**, 212 (1995).
- [16] Y. J. Kim and M. H. Cha, Int. J. Mod. Phys. E **13**, 439 (2004).
- [17] Y. J. Kim and M. H. Cha, Int. J. Mod. Phys. E **14**, 1051 (2005).
- [18] C.C. Sahn, T. Murakami, J.G. Cramer, A.J. Lazzarini, D. D. Leach, and D. R. Riger, R. A. Loverman, W.G. Lynch, M.B. Tsang, and J. Van der Plicht, Phys. Rev. C **34**, 2165 (1986).

근사된 Woods-Saxon 퍼텐셜을 이용한 Eikonal 위상이동과 $^{12}\text{C} + ^{208}\text{Pb}$ 탄성산란에의 적용

김 용 주

제주대학교 물리학과, 제주 690-756

근사된 Woods-Saxon 퍼텐셜에 기초한 쿨롱-수정된 eikonal 모형에서의 위상이동을 나타내었다. 이 위상이동은 $E_{\text{lab}} = 300 \text{ MeV}$ 와 420 MeV 인 $^{12}\text{C} + ^{208}\text{Pb}$ 계의 탄성산란 분석에 성공적으로 적용할 수 있었다.